Colloids and Surfaces B: Biointerfaces 81 (2010) 620–628

Contents lists available at ScienceDirect

Colloids and Surfaces B: Biointerfaces

journal homepage: www.elsevier.com/locate/colsurfb

# Copper, zinc, cadmium and lead biosorption by *Gymnogongrus torulosus*. Thermodynamics and kinetics studies

María Mar Areco, María dos Santos Afonso*

*INQUIMAE and Departamento de Química Inorgánica, Analítica y Química Física, Facultad de Ciencias Exactas y Naturales, Universidad de Buenos Aires, Ciudad Universitaria Pabellón II 3er Piso, C1428EHA Buenos Aires, Argentina*

ARTICLE INFO

*Article history:*
Received 30 April 2010
Received in revised form 14 July 2010
Accepted 6 August 2010
Available online 14 August 2010

*Keywords:*
Biosorption
Kinetics
Metal removal
*Gymnogongrus torulosus*

ABSTRACT

*Gymnogongrus torulosus* adsorption efficiency for cadmium(II), copper(II), lead(II) and zinc(II) were studied in batch mode in different acidic conditions. The adsorbent removal efficiency was determined as a function of contact time, initial metal ions concentration, pH and temperature. *G. torulosus* was characterized by SEM, water adsorption surface area and EDS. The Langmuir, Freundlich, Dubinin–Radushkevich and Temkin models have been applied and results showed that the biosorption process was better described by the Langmuir model. Kinetic experiments demonstrated that fast metal uptakes follow a pseudo-second-order kinetic model and that intra-particle diffusion and/or chemisorption were the rate-limiting steps. Experimental results show that *G. torulosus* isotherm followed the biosorption series, Cu > Cd ~ Zn ~ Pb.

Biosorption capacities were affected by solution parameters. The maximum metal uptake ($q_{max}$) increased with increasing pH. The affinity constant, $q_{max}$, and the pseudo-second-order kinetic constants were calculated for the adsorption of all studied metals onto *G. torulosus*. The Gibbs free energy of the adsorption process as well as the process enthalpy and entropy were calculated from experimental results.



## 1. Introduction

The increasing concentration of heavy metals in waters is mainly due to effluent discharges from industries. Pollution of natural waters by metal ions has become a major issue all over the world because metal concentrations in waters often exceed the admissible values. Consequently, industries are required to diminish the contents of heavy metals in their effluents to acceptable levels.

The increasing waste products are forcing scientist to study new and alternative technologies to remove trace metals from polluted waters [1] and one of the main goals regarding heavy metals removal from waste waters consists in the reduction of these pollutants at very low levels [2]

Biosorption, known as the sorption of heavy metals onto biological materials, is becoming a potential alternative for toxic metals removal from waters [3,4] and is a cost effective technology that uses readily available biomass from nature [5]. Among many biosorbents, marine seaweeds are excellent biosorbents for metals [6]. In recent years, the metal biosorption potential of various red, green and brown seaweeds were investigated by many researchers [7–13], and references therein.

Seaweeds have a high bonding affinity with heavy metals [1,14–20]. Since their cell walls have different functional groups (such as carboxyl, hydroxyl, phosphate or amine) that can bind to metal ions [21], they are much more efficient than active carbon and natural zeolites and, depending on the pH, these groups are either protonated or deprotonated [22,23].

Many works describing metals biosorption have been published [8,24–30]. The advantages of using dried aquatic algae for metal removal derive from its high efficiency as biosorbents, easy handling, no nutrient requirements, low costs, and their availability.

*Gymnogongrus torulosus* (Rhodophyta) is a seaweed with great commercial interest in Argentina because it produces carrageenan, a polysaccharide commonly used in hydrocolloid industries. This seaweed predominates along the coastal and continental shelf areas of temperate and cold-water regions. Thus, the present study was focused on heavy metal removal from aqueous solution by *G. torulosus* under different experimental conditions in order to optimize the efficiency of the adsorption process. Equilibrium isotherm and kinetic models were carried out for a better understanding of the adsorption process.

* Corresponding author. Tel.: +54 11 4576 3378/80x125; fax: +54 11 4576 3341.
*E-mail address:* dosantos@qi.fcen.uba.ar (M. dos Santos Afonso).

0927-7765/$ – see front matter © 2010 Elsevier B.V. All rights reserved.
doi:10.1016/j.colsurfb.2010.08.014

## 2. Materials and methods

### 2.1. Biosorbent material

*G. torulosus* were collected in Cabo Corrientes at Mar del Plata City, Buenos Aires Province, Argentina. The seaweed was washed thoroughly with deionized water, then dried overnight at 60 °C and finally stored in desiccators before being used. Afterwards, the dried seaweed was blended in a homogenizer into finer particles. A stainless steel standard sieve was used to obtain fine particles (0.5–2 mm) of seaweed, which were subsequently used for biosorption experiments.

The specific surface area was determined by water adsorption at room temperature ($S_w$ = 312.2 $m^2\ g^{-1}$) [31,32]. Seaweeds particles were kept, until a constant weight was attained, in a desiccators containing a saturated solution of $Ca(NO_3)_2{\cdot}6H_2O$ that ensures a relative humidity of rh = 0.56.

Dehydrated raw and adsorbed metal samples were fixed to 10 mm metal mounts using carbon tape and spit coated with gold under vacuum in an argon atmosphere. The surface morphology of the coated samples was visualized by a file emission gun scanning electron microscope Zeiss (FEG-SEM Zeiss LEO 982 GEMINI) with combined energy dispersive X-ray analyzer (EDS) at a voltage of 3.0 kV. SEM permitted the identification of interesting structural features on the seaweed surface with EDS. INCA software was used to determine the elemental composition of the surface before and after metal binding.

### 2.2. Metal solutions

All chemicals used were of analytical reagent grade and were used without further purification. All solutions and algal suspensions were prepared using Milli-Q water with a resistivity of 18.0 MΩ cm.

Stock zinc(II), copper(II), cadmium(II) and lead(II) solutions for the experiments were prepared by dissolving $ZnSO_4{\cdot}7H_2O$, $CuSO_4{\cdot}5H_2O$, $Cd(NO_3){\cdot}4H_2O$ and $Pb(NO_3)$ respectively. All solution concentrations ranged from 25 to 500 mg $l^{-1}$ of each metal.

### 2.3. Experimental procedure

#### 2.3.1. Batch experiments

The metal sorption performances for Cu(II), Zn(II), Cd(II) and Pb(II) in batch mode by *G. torulosus* were compared. Batch sorption experiments were performed with 0.1 g of biomass suspended in 100 ml of Zn(II), Cu(II), Cd(II) or Pb(II) solutions in a concentration range between 25 and 500 mg $l^{-1}$ of each metal. Suspensions were kept in constant agitation at desired and constant pH and temperature. Experiments were carried out by triplicate for each concentration.

Algal biomass was separated from metal solutions by filtration with cellulose nitrate membrane filters (0.22 μm pore). Afterwards, the final metal concentrations in the filtered solutions were determined and metal uptake ($q$) was calculated using the following mass balance equation [7]

$$q = \left[\frac{(C_i - C_{eq}) \times V}{m}\right] \quad (1)$$

where $C_i$ is the initial metal concentration (mg $l^{-1}$ or mM), $C_{eq}$ the equilibrium metal concentration (mg $l^{-1}$ or mM), $V$ the solution volume (l) and $m$ is the dry seaweeds weight (g).

The dissolved metal removal efficiency (RM, %) by both biosorbents was determined by the following equation:

$$RM = \left[\frac{(C_i - C_{eq}) \times 100}{C_i}\right] \quad (2)$$

Control experiments were carried out in the absence of adsorbents in order to find out whether there is any adsorption on the container walls.

#### 2.3.2. Effect of pH

The pH dependence of metal uptake by *G. torulosus* was studied through batch experiments in a pH range from 1 to 6, with 1 g $l^{-1}$ algae concentration and Pb(II), Cd(II), Cu(II) and Zn(II) initial concentration of 0.21, 0.45, 0.77 and 0.90 mM, respectively. The pH range was selected in order to avoid metal (hydr)oxides precipitation, and to ensure that the decay of metal concentration is due to adsorption processes. The pH was adjusted using 0.1 M HCl or 0.1 M NaOH. The biosorption experiments were carried out by triplicate and there were no significant differences within each triplicate. The expressed values represent the average of the obtained results. Resulting pH was measured using a Metrohm 644 pH-meter with a combined glass microelectrode.

### 2.4. Metal quantification

Cadmium(II) and lead(II) concentrations were determined by atomic absorption spectroscopy (AAS) using a Shimadzu 6800 spectrophotometer with a GF-6501 graphite oven, an ASC-6000 autosampler Hamamatshu and lead(II) and cadmium(II) cathode lamps.

Zinc(II) concentrations were spectrophotometrically measured at 620 nm wavelength using Zincon (2-carboxy-2′-hydroxy-5′-sulfoformacylbenzol) as a chromogenic reagent. Zinc–Zincon blue complex is formed at pH values between 8.5 and 9.5 [33].

Copper(II) concentrations were spectrophotometrically measured using 1 g of Sodium Diethyldithiocarbamate (DDTC) dissolved in ethanol–water 50% (v/v) and $H_2SO_4$ ($10^{-3}$ M), as reagent [29]. At low pH DDTC forms a yellow complex with copper(II). Absorbance of the corresponding solution was measured at 440 nm.

Absorbance measurements were made with a double beam UV–vis spectrophotometer Shimadzu-Pharmaspec UV-1700 and a 1 cm path length quartz cuvette.

### 2.5. Reproducibility and data analysis

Unless otherwise indicated, all data shown are the mean values from three replicate experiments. Standard deviations were below 5%.

The statistical data analyses were made using the SigmaPlot software package. SigmaPlot uses the Durbin–Watson statistic to test residuals for their independence of each other. The Durbin–Watson statistic is a measure of serial correlation between the residuals. The residuals are often correlated when the independent variable is time, and the deviation between the observation and the regression line at one time is related to the deviation at the previous time.

## 3. Results and discussion

### 3.1. Biosorption kinetics

Equilibrium analysis is fundamental in order to evaluate the affinity or capacity of a sorbent. However, it is important to assess how sorption rates vary with aqueous free metal concentrations, and how rates are affected by sorption capacity or by the sorbent

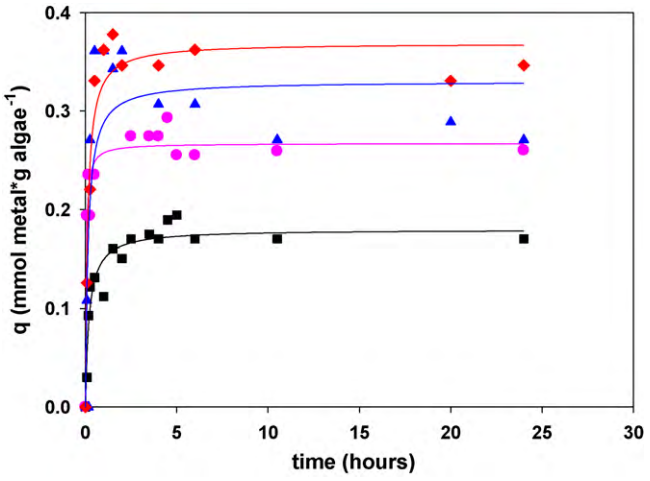


**Fig. 1.** Biosorption kinetics of metal uptake at pH 5.5 and room temperature for (♦): Cu(II); (▲): Zn(II); (■): Pb(II) and (●): Cd(II) biosorbed onto *G. torulosus*. Solid lines were calculated using binding ligand kinetics model with parameters showed in Table 1.

character in terms of kinetics [34]. Fig. 1 shows the four metal uptakes by *G. torulosus* versus time at pH 5.5 and room temperature. The initial metal concentrations were 0.99; 0.83, 0.360 and 0.350 mM of Zn(II), Cu(II), Cd(II) and Pb(II), respectively. The metal uptake was calculated using Eq. (1) and increases with the time of contact, it is relatively fast and in less than 5 h the equilibrium plateau is reached. Thus, metal uptake was faster for the first 3 h and afterwards the adsorption rates slowed until attaining equilibrium.

The equilibration time for maximum uptake is reached in less than 5 h and an equilibration period of 24 h was selected for adsorption experiments. The time profile of metal uptake is a single, smooth, and continuous curve leading to saturation, suggesting the possible monolayer coverage on the surface of the adsorbent. Three kinetic models, pseudo-first-order, pseudo-second-order and intra-particle diffusion were applied in order to interpret the experimental results.

### 3.1.1. Kinetic models

The extent of biosorption is only dependent on the initial and final equilibrium states. The biosorption rate is dependent on the way that the process is performed between the initial and final steps. Sorption kinetics may be controlled by several independent processes such as transport from the bulk to the surface and chemical binding reactions of the sorbate.

Surface complex formation with metal ions involves the coordination of metal ions with oxygen donor atoms that constitute the biomasses cell walls, followed by the release of protons from the surface. For example:

$$\equiv SOH + Me^{2+} \underset{k_b}{\overset{k_f}{\rightleftarrows}} \equiv SOMe^{+} + H^{+} \quad (3)$$

where $Me^{2+}$ is the concentration of sorbate in solution, ≡SOH is the sorbent surface site which is susceptible of coordination, $\equiv SOMe^{+}$ is the sorbate concentration on the sorbent at any time, and $k_f$ and $k_b$ are the kinetic constants for the forward and backward reaction steps.

Usually, the transport process in the bulk solution and the film diffusion through the boundary layer of bioadsorbent are considered fast processes. Therefore, intra-particle diffusion or chemical binding reactions are the controlling steps of the adsorption mechanism.

*3.1.1.1. Pseudo-first-order model.* The most widely used kinetic model for biosorption is a first order reversible kinetic model that was previously reported by Bhattacharya and Venkobachar [35]. They presented a model based on concentration solution and on cadmium(II) sorption by establishing a balance between liquid phase and solid biomass.

The pseudo-first-order kinetics model was applied to many systems, from organic compounds, such as dyes, to heavy metals adsorbed on biomaterials, biopolymers or on solid inorganic matrices [36]. This kinetic model is based on a pseudo-first-order rate expression of Lagergren

$$\ln(q_e - q_t) = \ln q_e - k_1 t \quad (4)$$

where $k_1$ is the pseudo-first-order sorption rate constant, $q_e$ is the amount of metal ion adsorbed at equilibrium by the biomass and $q_t$ is the amount of metal ion adsorbed at any time $t$. Both, $q_e$ and $q_t$ were expressed in mmol $g^{-1}$ units. The overall rate constant $k_1$, in $h^{-1}$, was calculated from the slope by plotting $\ln(q_e - q_t)$ versus $t$ (Table 1). The correlation coefficients using the Lagergren model obtained at all studied initial concentrations were relatively low, ranging from 0.1393 to 0.7280 for all studied metals. Moreover, the experimental $q_e$ values did not agree with the calculated data. This suggests that the adsorption of lead(II), cadmium(II), zinc(II) and copper(II) onto *G. torulosus* can not be considered as a pseudo-first-order kinetic.

*3.1.1.2. Pseudo-second-order model.* Since the pseudo-first-order model is not applicable for the understanding of the adsorption kinetics of heavy metals on *G. torulosus* biomass, the pseudo-second-order model was tested. In this model the rate at which adsorption sites are covered is proportional to the square of the number of unoccupied sites, and the number of occupied sites is proportional to the fraction of the metal ion adsorbed. Several systems respond to a second order kinetics model for sorption

**Table 1**
Intra-particle diffusion, pseudo-first-order and pseudo-second-order kinetic parameters for four metals at room temperature and pH 5.5. $q_{eq}$: maximum coverage concentration, $k_1$: pseudo-first-order constant, $k_2$: pseudo-second-order constant, $k_{id}$: intra-particle diffusion constant.

| Me | | Zn | Cu | Pb | Cd |
|---|---|---|---|---|---|
| Pseudo-first-order | $q_e$ (mmol $g^{-1}$) | 0.09 | 0.08 | 0.11 | 0.11 |
| | $k_1$ ($h^{-1}$) | 0.46 | 0.35 | 0.41 | 0.40 |
| | $R^2$ | 0.1393 | 0.2040 | 0.7280 | 0.6185 |
| Pseudo-second-order | $q_e$ (mmol $g^{-1}$) | 0.28 | 0.34 | 0.17 | 0.26 |
| | $k_2$ (g $h^{-1}$ $mmol^{-1}$) | 87.83 | 71.91 | 142.19 | 93.84 |
| | $R^2$ | 0.9972 | 0.9989 | 0.9979 | 0.9991 |
| Intra-particle diffusion | $k_{id}$ (mmol $h^{-1}$ $g^{-1}$) | 0.42 | 0.38 | 0.21 | 0.32 |
| | $R^2$ | 0.7320 | 0.9584 | 0.8918 | 0.7387 |

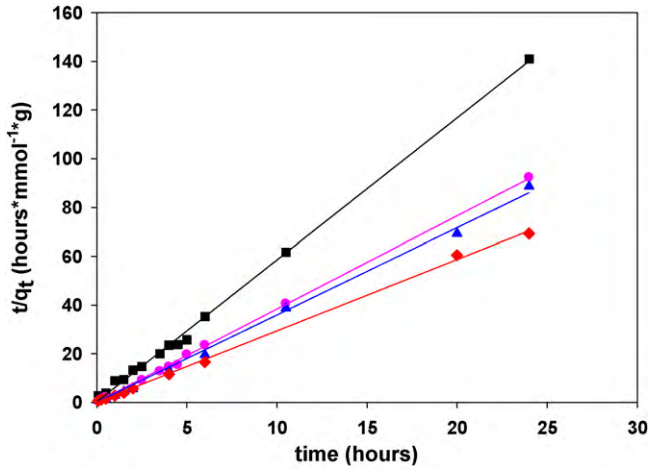


**Fig. 2.** Pseudo-second-order kinetics model for the biosorption of (◆): Cu(II); (▲): Zn(II); (■): Pb(II) and (●): Cd(II) onto *G. torulosus*.

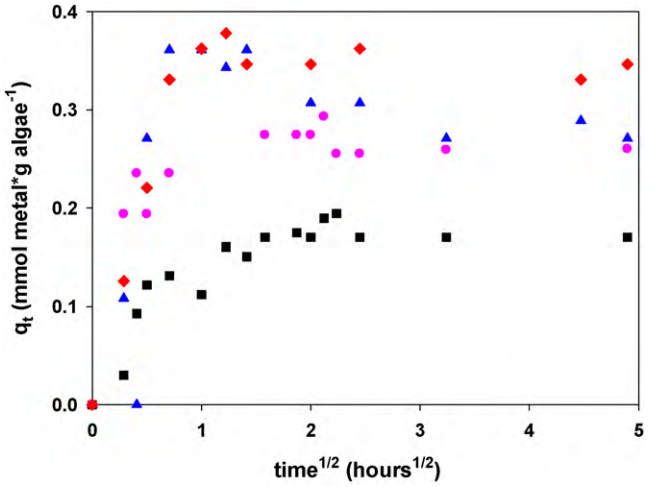


**Fig. 3.** Intra-particle diffusion kinetics model for the biosorption of (◆): Cu(II); (▲): Zn(II); (■): Pb(II) and (●): Cd(II) onto *G. torulosus*.

reactions, and are represented by the following equation [36]:

$$\frac{dq_t}{dt} = k_2(q_e - q_t)^2 \quad (5)$$

where $k_2$ is the rate of pseudo-second-order adsorption and $q_e$ and $q_t$ are the amount of metal ion adsorbed at equilibrium and the amount adsorbed at any time, respectively. The sorption rate can be calculated as the initial sorption rate when $t$ approaches 0. Integrating and rearranging, the pseudo-second-order equation can be written as:

$$\frac{t}{q_t} = \frac{1}{k_2 q_e^2} + \frac{t}{q_e} \quad (6)$$

where $k_2$ is the rate constant of the pseudo-second-order sorption.

The linear plot of $t/q_t$ against $t$ was made in order to calculate the second order rate constant $k_2$ and the equilibrium adsorption capacity $q_e$ from the slope and intercept, respectively, as represented in Fig. 2.

The solid lines in Figs. 1 and 2 were plotted using the binding ligand model (Eq. (7)) and the pseudo second-order kinetics (Eq. (6)), respectively. The parameters obtained are listed in Table 1. The binding ligand model is represented by Eq. (7):

$$q = \frac{B_{max} \times t}{(k + t)} \quad (7)$$

Eq. (7) is equivalent to Eq. (6) when $B_{max} = q_e$ and $k_2{}^{-1} = k \times B_{max}$. Figs. 1 and 2 and Table 1 show significant agreement between the experimental and the calculated values. The fitting parameters for both pseudo-first and pseudo-second-order equations are listed in Table 1. The correlation factors of the pseudo-second-order kinetics model varied between 0.9972 and 0.9991 showing that pseudo-second-order model accurately represents the experimental behavior.

The analysis of the results shows that the correlation factors obtained are not so good for the pseudo-first-order model, while results obtained for the pseudo-second-order kinetic model were very good. Moreover, the values of $q_e$ calculated from the pseudo-first-order kinetics are not similar to the experimental values, while those calculated from second-order model are in good agreement with the experimental values in Fig. 1. Thus, it is clear that experimental data are better fitted by the second order equation than by the pseudo-first-order equation.

The pseudo-second-order model has already been successful applied to the description of Cd(II), Cu(II), Ni(II), Pb(II) biosorption by different bioadsorbents. The obtained pseudo-second-order kinetic parameters are in accordance with those found in the literature [34,36–38].

*3.1.1.3. Intra-particle diffusion model.* The surfaces of an algae cell or a mineral particle suspended in water have interface boundaries that are characterized by a discontinuity of certain parameters such as density and chemical composition. The intrinsic adsorption is often faster than the transport to the interface. The thickness of the boundary layer surrounding the particle should be minimal when agitation speed will be fast enough and boundary layer resistance or film diffusion should not be a rate-controlling step.

The rate constant for intra-particle diffusion ($k_{id}$) is given by

$$q_t = k_{id}(t)^{1/2} \quad (8)$$

where $k_{id}$ is the internal diffusion coefficient, $q_t$ the amount of metal adsorbed at time $t$ and $t$ the sorption time. Plots of $q$ versus $t^{1/2}$ for lead(II), cadmium(II), zinc(II) and copper(II) are shown in Fig. 3. From this figure, an initial steep-sloped portion at intra-particle diffusion is seen, followed by the plateau at equilibrium. The initial segment of the curve with a sharp slope (from 0 to 1 h) is attributed to surface adsorption, where the intra-particle diffusion is the rate-controlling step followed by a plateau that corresponds to equilibrium. The intra-particle diffusion rate was obtained from the slope of the linear part of the curve.

The correlation coefficients were not so good ($R^2$ values ranged from 0.7320 to 0.9584, see Table 1). The straight lines obtained in the linear portion of the plot did not pass through the origin, indicating that pore diffusion was not the only controlling step. This deviation from the origin may be due to the difference in the rate of mass transfer in the initial and final stages of adsorption. This indicates some degree of boundary layer control and further show that the intra-particle diffusion was not the only rate-limiting step, chemical binding may also control the rate of sorption, or both process may operate simultaneously.

The correlation coefficients for the pseudo-second-order kinetic model are greater than those for the intra-particle diffusion model (Table 1), suggesting a chemical reaction mechanism [39]. This would indicate that the metal cations sorption is a complex mix of surface chemisorption occurring on the boundary layer of the algal particle and intra-particle diffusion.

*3.1.1.4. Temperature effect.* Temperature can influence the sorption process rate. An increase in temperature from 7 to 25 °C at pH 5.5 increases the pseudo-second-order kinetic constant by a factor of 2.1, 17.3, 13.6 and 10.5 for lead(II), cadmium(II), zinc(II)

and copper(II), respectively. Increasing the temperature from 25 to 55 °C decreases the pseudo-second-order kinetic constant by a factor of 0.1, 0.2 and 0.6 for lead(II), cadmium(II) and copper(II), respectively, and increases the constant by a factor of 1.1 for zinc(II) probably caused by a change in the texture of the sorbent and a loss in the sorption capacity due to material deterioration [5].

### 3.2. Sorption models

Adsorption isotherms are important criteria in optimizing the use of adsorbents materials because they describe the nature of the interaction between sorbate and adsorbent. Thus, analysis of experimentally obtained equilibrium data by either theoretical or empirical equations is useful for practical design and operation of adsorption systems.

There are a great number of expressions that describe adsorption isotherms. Here the Langmuir, Freundlich, Dubinin–Radushkevich and Temkin models were applied to the equilibrium data.

#### 3.2.1. Langmuir adsorption isotherms

The Langmuir isotherm is a well-known model that indicates a reduction of the available interaction places as the metal ion concentration increases. The Langmuir isotherm assumes monolayer adsorption and is determined by the following equation:

$$q = \frac{q_{\max} \times K_L \times C_{eq}}{(1 + K_L \times C_{eq})} \quad (9)$$

where $q_{\max}$ is the maximum metal uptake (in mg g$^{-1}$ or mmol g$^{-1}$), meaning the maximum concentration on the solid phase, $C_{eq}$ is the metal concentration at the equilibrium on the aqueous media and $K_L$ is the Langmuir equilibrium constant which is related with the free energy of the reaction.

Copper(II), zinc(II), cadmium(II) and lead(II) adsorption isotherms for *G. torulosus* are presented in Fig. 4. The Langmuir isotherm, Eq. (9), was applied to estimate seaweed adsorption capacity. The Langmuir parameter and the correlation factor for the four metals are indicated in Table 2. Affinity between sorbent and sorbate are represented by the constant $K_L$. In general good biosorbents have a high $q_{\max}$ and a high $K_L$. *G. torulosus* have high saturation ($q_{\max}$) for all metals studied, except for lead(II). The maximum coverage, $q_{\max}$, follow the sequence Cu > Cd > Zn > Pb.

The solid lines in Fig. 4 where plotted with the Langmuir model applied to metal uptake during the sorption process. The calculated lines and the experimental data match very well. The maximum adsorption capacities are one order in magnitude higher than those listed in [40] for different biosorbents.

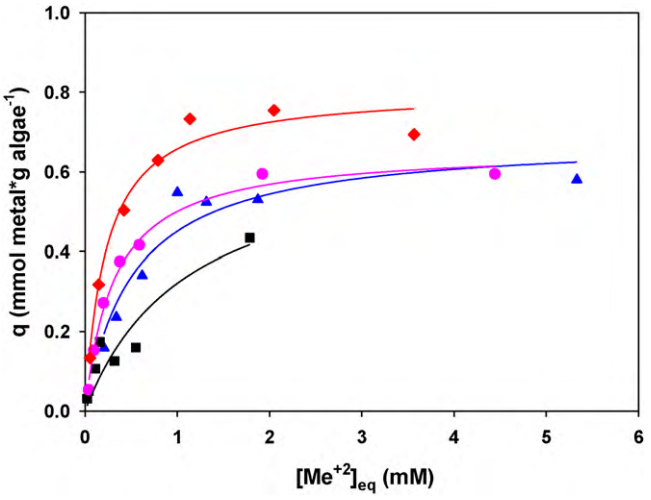


**Fig. 4.** Adsorption isotherms at pH 5.5 for *G. torulosus*, (♦): Cu(II); (▲): Zn(II); (■): Pb(II) and (●): Cd(II). Solid lines were calculated using Langmuir model.

#### 3.2.2. Freundlich adsorption isotherms

The Freundlich isotherm assumes a heterogeneous surface with a nonuniform distribution of heat of adsorption over the surface. Thus the Freundlich model describes the adsorption on an energetically heterogeneous surface on which the adsorbed molecules are interactive. This isotherm is represent by Eq. (10)

$$q_e = K_F \times C_{eq}^{1/n} \quad (10)$$

where $K_F$ is the Freundlich constant indicating adsorption capacity and $1/n$ is the adsorption intensity. Linear regression analysis was used for isotherm data treatment. The linear form of the Freundlich isotherm used was

$$\ln q_e = \ln K_F + \left(\frac{1}{n}\right) \times \ln C_{eq}$$

The values of $K_F$ and $1/n$ were calculated from the intercept and slope of the plot between $\ln q_e$ versus $\ln C_{eq}$. $K_F$, $1/n$ and the correlation coefficient ($R^2$) values of the Freundlich isotherm are given in Table 2.

For all cases, the Langmuir equation fits the experimental data better than the Freundlich equation. This isotherm does not predict any saturation of the adsorbent by the sorbate. Instead, infinite surface coverage is predicted, indicating multilayer sorption on the surface.

**Table 2**
Fitting parameters for Langmuir, Freundlich, Temkin and Dubinin–Radushkevich isotherm equations.

| Me | Langmuir $q = \frac{q_{\max} K_L C_e}{(1+K_L C_e)}$ | | | Freundlich $q = K_F C_e^{1/n}$ | | |
|---|---|---|---|---|---|---|
| | $q_{\max}$ (mmol g$^{-1}$) | $K_L$ (l mmol$^{-1}$) | $R^2$ | $K_F \times 10^{-03}$ | $1/n$ | $R^2$ |
| Zn | 0.68 ± 0.056 | 1.93 ± 0.39 | 0.9080 | 6.89 | 0.41 ± 0.09 | 0.8013 |
| Cu | 0.81 ± 0.037 | 4.40 ± 0.88 | 0.9716 | 9.12 | 0.40 ± 0.07 | 0.8648 |
| Pb | 0.68 ± 0.23 | 0.90 ± 0.40 | 0.9226 | 12.51 | 0.54 ± 0.08 | 0.9035 |
| Cd | 0.66 ± 0.021 | 3.18 ± 0.32 | 0.9904 | 12.81 | 0.49 ± 0.10 | 0.8364 |

| Me | Temkin $q = B \times \ln K_T + B \times \ln C_e$ | | | Dubinin–Radushkevich $\ln q = \ln q_{\max} - \beta\varepsilon_o^2$ | | |
|---|---|---|---|---|---|---|
| | $K_T$ (l mg$^{-1}$) | $B$ (mg g$^{-1}$) | $R^2$ | $q_{\max}$ (mmol g$^{-1}$) | $-\beta \times 10^{-04}$ | $R^2$ |
| Zn | 0.309 | 9.31 ± 1.86 | 0.8333 | 0.504 | 88.0 ± 15 | 0.8618 |
| Cu | 0.938 | 9.65 ± 1.29 | 0.9168 | 0.611 | 7.0 ± 1 | 0.8609 |
| Pb | 0.200 | 16.2 ± 3.9 | 0.7685 | 0.164 | 2.0 ± 0.05 | 0.6470 |
| Cd | 0.357 | 14.1 ± 1.1 | 0.9703 | 0.403 | 7.0 ± 1 | 0.8345 |

**Table 3**
Thermodynamics parameters for the adsorption of Zn(II), Cu(II), Pb(II) and Cd(II) on *G. torulosus* at pH 5.5 and room temperature.

| Me | Langmuir | Temkin | | Dubinin–Radushkevich | Thermodynamic parameters | | |
|---|---|---|---|---|---|---|---|
| | $\Delta G_{ads}$ (kJ mol$^{-1}$) | $b$ (J mol$^{-1}$) | $\Delta G_{ads}$ (kJ mol$^{-1}$) | $E$ (kJ mol$^{-1}$) | $\Delta G^{\circ}$ (kJ mol$^{-1}$) | $\Delta H^{\circ}$ (kJ mol$^{-1}$) | $\Delta S^{\circ}$ (J mol$^{-1}$) |
| Zn | −18.74 | 266 | −24.56 | 7.54 | −10.44 | 28 | 129 |
| Cu | −20.78 | 257 | −27.24 | 26.73 | −15.64 | −33 | −59 |
| Pb | −16.86 | 153 | −26.33 | 50.00 | −15.25 | −24 | −32 |
| Cd | −19.98 | 175 | −26.26 | 26.73 | −15.65 | −23 | −25 |

### 3.2.3. Dubinin–Radushkevich adsorption isotherms

Dubinin and Radushkevich proposed a well-liked equation for the analysis of isotherms in order to determine if the adsorption occurred by a physical or chemical process. The D–R equation is more general than the Langmuir model because it does not assume a homogeneous surface, a constant sorption potential nor absence of steric hindrance between adsorbed and incoming particles

$$\ln q_e = \ln q_{max} - \beta\varepsilon^2 \quad (11)$$

where $q_e$ is the amount of metal cations adsorbed per g of biomass, $q_{max}$ represents the maximum sorption capacity of the adsorbent, $\beta$ is a constant related to sorption energy (D–R constant) and $\varepsilon$ is the Polanyi sorption potential calculated by Eq. (12)

$$\varepsilon = RT \ln\left(1 + \frac{1}{C_{eq}}\right) \quad (12)$$

where $R$ is the gas constant 8.314 J mol$^{-1}$ K$^{-1}$, $T$ is the temperature in Kelvin and $C_{eq}$ is the metal equilibrium concentration. The Polanyi sorption approach assumes a fixed volume of sorption space close to the adsorbent surface and the existence of sorption potential over these spaces. The sorption space in the vicinity of a solid surface is characterized by a series of equipotential surfaces having the same sorption potential. This sorption potential is independent of the temperature but varies according to the nature of sorbent and sorbate.

The values of $\beta$ and $q_{max}$ were calculated from the slope and the intercept of the plot of $\ln q_e$ versus $\varepsilon^2$ (Table 2). The mean free energy of sorption per molecule of sorbate required to transfer one mole of ion from the infinity in the solution to the surface of biomass and can be determined by the following Eq. (13)

$$E = (-2\beta)^{-1/2} \quad (13)$$

The Dubinin–Radushkevich constants calculated for the adsorption by *G. torulosus* of all metals studied are shown in Table 2.

All energy values obtained (Table 3) have $E > 8$ kJ mol$^{-1}$, which indicate that all metal cation adsorptions were chemical processes, since a physical adsorption process has an $E < 8$ kJ mol$^{-1}$. The sorption capacity was lower than the sorption capacity calculated using the Langmuir model, which may be attributed to different assumptions taken into consideration. From comparing the correlation coefficient values, it was concluded that the sorption of lead(II), cadmium(II), zinc(II) and copper(II) onto *G. torulosus* biomass followed the Langmuir model.

### 3.2.4. Temkin adsorption isotherms

The Temkin isotherm is represented by the following equation:

$$q_e = \frac{RT}{b} \ln(k_T C_e) = B \ln(k_T C_e) \quad (14)$$

where constant $B = RT/b$ is related to the heat of adsorption, $R$ is the universal gas constant (J mol$^{-1}$ K$^{-1}$), $T$ is the temperature (K), $b$ is the variation of adsorption energy (J mol$^{-1}$) and $K_T$ is the equilibrium binding constant (l mg$^{-1}$) corresponding to the maximum binding energy. The Temkin isotherm assumes that the heat of adsorption of all the molecules in a layer decreases linearly due to adsorbent–sorbate interactions and that adsorption is characterized by a uniform distribution of binding energies, up to some maximum binding energy. A plot of $q_e$ versus $\ln C_e$ makes possible the determination of the isotherm constants $B$ and $K_T$ from the slope and the intercept, respectively. The calculated values for Temkin parameters are shown in Table 2. The correlation factors show that the Langmuir model approximation to the experimental results is better than the Temkin model. Consequently, among the four isotherm models used, the Langmuir model offers the best correlation factors.

Experimental results show that *G. torulosus* isotherm follows the biosorption series, Cu > Cd ~ Zn ~ Pb, while the sequence obtained for $K_L$ values (Table 2) is Cu > Cd > Zn > Pb. These results show that copper has the highest affinity for cell wall functional groups.

Studies carried out using *Sargassum fluitans* showed a decrease in metals uptake when carboxylic groups – COO – are blocked due to esterification processes [41]. Similar results were also obtained for carboxyl groups of fresh water biomass such as *Chlorella pyrenoidosa* and *Cyanidium caldarium* [42]. The hydroxyl groups are also present in all polysaccharides but they are less abundant at low pH values, increasing their contribution to metallic cation adsorption at basic pH.

Scanning electron microscope (SEM) images were used for the surface analysis of *G. torulosus* as shown in Fig. 5. The SEM images

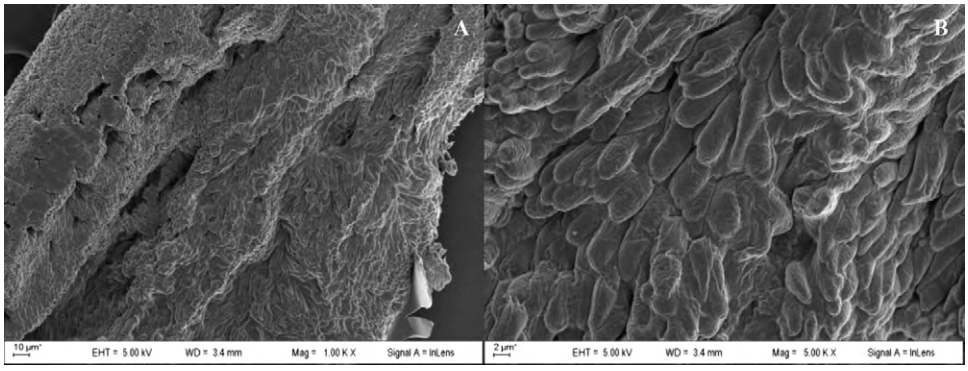


**Fig. 5.** *G. torulosus* Scanning Electron Microscopy (SEM) at different magnification (A: 1000× and B: 5000×) and 5.0 kV.

were taken by applying 5 kV voltage with different magnification times for the clarification of surface. These figures demonstrate the fibrous superficial structure of the algal biomass surface where the metal cations could be adsorbed. The EDS images for the seaweed before and after adsorption are presented in Fig. 6 and show the metal cations adsorbed on the algae surface.

Biosorbent capacity has been mainly attributed to properties of the cell wall, a structure of fibers absorbed in an amorphous matrix of polysaccharides. *G. torulosus* contain cellulose in the inner cell wall with the outer cell wall consisting of an amorphous embedding matrix [43] that is made by xylans and several sulfated galactans including agar and carrageenan. The polysaccharides are important components of the cell wall and they can either coexist in it or be part of the intracellular or extracellular polymeric substances containing ionisable functional groups such as carboxyl, phosphoric, amine, and hydroxyl groups [43]. These functional groups represent potential binding sites for the sequestration of metal ions [43,44]. They can constitute up to 40% of the dry matter and have a great affinity for divalent cations [45]. Also, the incorporation of trivalent cations has been attributed to the presence of sulfated polysaccharides [46]. Therefore the differences in zinc(II), cadmium(II), copper(II) and lead(II) biosorption can be attributed to the polysaccharides present in the algae cellular walls probably because these organic compounds may have different affinities for each metal.

Stumm and Morgan [47] have suggested that for alkaline and alkaline earth metals the tendency of cations to be adsorbed increase with the ionic radius of the ion. Copper and zinc sequences also follow the Irving–Williams order that may be explained by considering factors such as effective nuclear charge, ionic radii, ligand field stabilization, and the Jahn–Teller effect. Essentially, the +2 oxidation state complexes of the first transition series become more stable as the size of the metal ion decreases, although there are other effects arising from crystal/ligand field theory. Coordination complexes stability increases from calcium to copper and furthermore decreases with zinc, indicating that the coordination complexes of zinc are less stable than copper complexes. The tendency to form surface complexes, such as those formed between seaweeds and metals, may be compared with the tendency to form corresponding inner-sphere solute complexes [47]. When the relation between $K_L$ and the aqueous metal sulfate complex formations is compared a simultaneously growth is found. Instead, for hydroxyl groups the surface metal complex formations constants follow an inverse behavior compared with the aqueous metal hydroxyl complex formations constants. These results indicate that sulfated groups are the main coordination centers on cell walls.

### 3.2.5. Thermodynamic study

Thermodynamic parameters were calculated to confirm the adsorption nature of the present study. The thermodynamic constants, free energy change ($\Delta G^\circ$), enthalpy change ($\Delta H^\circ$) and entropy change ($\Delta S^\circ$) were calculated to evaluate the thermodynamic feasibility of the process and to confirm the nature of the adsorption process.

The Gibbs adsorption process, free energy, as well as, the enthalpy process was calculated from experimental results using the following equations

$$\Delta G^\circ = -RT \ln K \quad \text{and} \quad \Delta G^\circ = \Delta H^\circ - T\Delta S^\circ$$

where $R$ is the universal gas constant ($8.314\,\mathrm{J\,mol^{-1}\,K^{-1}}$), $T$ is the temperature in Kelvin and $K$ is the equilibrium constant, calculated as the surface and solution metal distribution ratio ($K = q_e/C_e$). All values obtained are summarized in Table 3. The $\Delta G^\circ$ values calculated are close to those obtained using the Langmuir affinity constant and differ from those obtained using the Temkin model constants. Negative values of $\Delta H^\circ$ suggest the exothermic nature

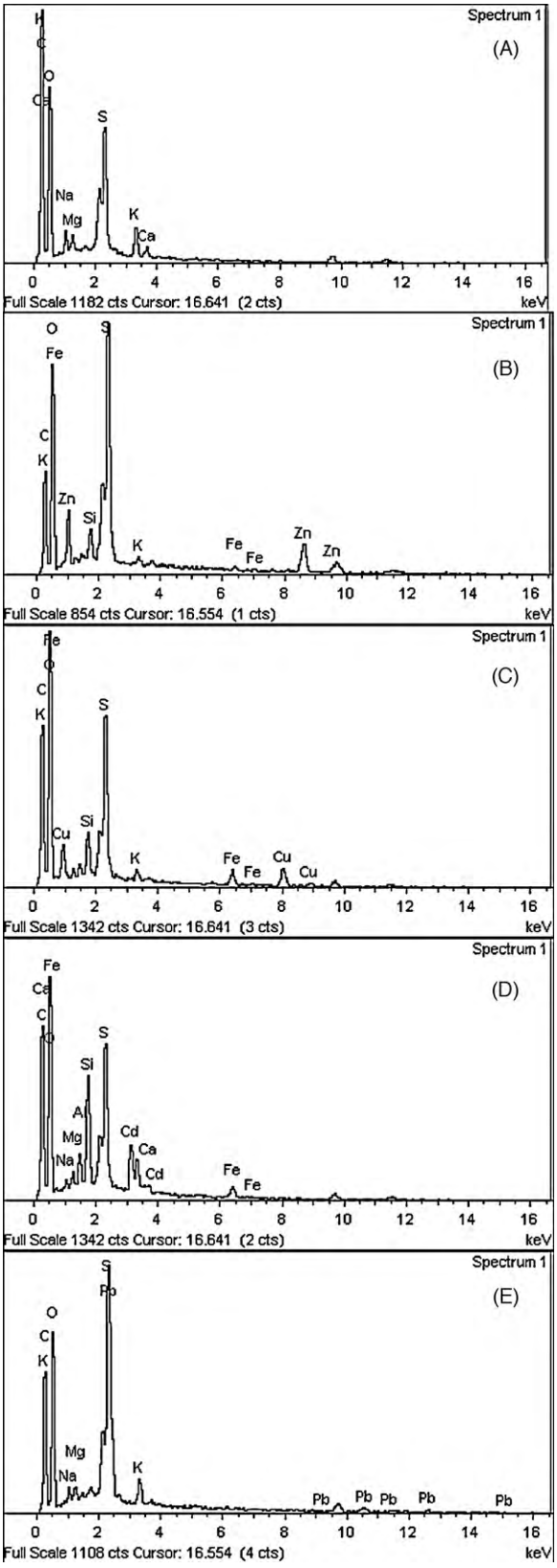


**Fig. 6.** EDS images for *G. torulosus:* (A) before treatment, (B), (C), (D) and (E) after the adsorption of Zn, Cu, Cd and Pb respectively

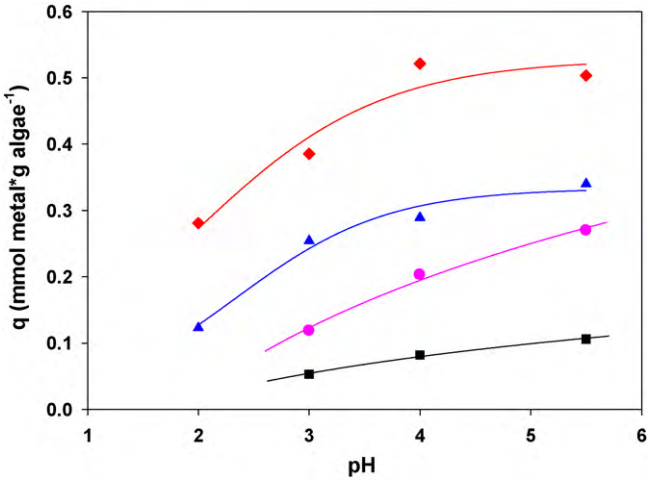


**Fig. 7.** *G. torulosus* biosorption experiments as function of pH, (♦): Cu(II); (▲): Zn(II); (■): Pb(II) and (●): Cd(II).

of the adsorption and the negative values of $\Delta G^{\circ}$ indicate the spontaneous nature of the adsorption process. However, the negative value of $\Delta G^{\circ}$ decreases with an increase in temperature, indicating that the spontaneous nature of adsorption is inversely proportional to the temperature. The negative values of $\Delta S^{\circ}$ show the decrease in randomness at the solid/solution interface during the adsorption process.

### 3.3. Metal recovery

*G. torulosus* removal efficiencies, at pH 5.5 and room temperature, are 74.28%, 48.57%, 42% and 27.27% for Cd(II), Pb(II), Cu(II) and Zn(II) respectively. The recovery values stated in this study are higher than the values reported in literature for other biomass materials [10,11,20]. This is probably due to the differences on the cell wall structure attributed to the polysaccharides present in the *G. torulosus* cellular walls that have different affinities for each metal as was mentioned before.

### 3.4. Influence of pH

The influence of solution pH on *G. torulosus* biosorption capacity was studied (Fig. 7) in a series of batch biosorption experiments. *G. torulosus* shows a similar behavior for all metal biosorptions between the pH ranges studied. Lead biosorption exhibits a slight dependence on pH. Both zinc(II) and copper(II) have a similar profile with a higher dependence on pH, while cadmium shows a moderate pH dependence.

Initial solution pH plays a significant role on metal biosorption, with maximum uptake at pH values above 5. In acidic conditions, the functional groups of the cell walls are protonated, which means that the majority of the binding sites are occupied by protons therefore decreasing the seaweed metal biosorbent capacity.

Metal biosorption dependence on pH is also related to the chemical speciation of the metals in solution.

The typical metal sorption dependence on pH suggests that carboxilic groups of algae cell walls are the most probable adsorption sites. These algae cell wall functional groups play an important role in metal binding at different pH conditions [48].

## 4. Conclusions

Experimental evidence suggests that the biomass of *G. torulosus* could be used as an efficient biosorbent for the removal of Zn(II), Cu(II), Pb(II) and Cd(II) ions. The initial pH significantly influenced metal uptake. Biosorption kinetics follows a pseudo-second-order model. Experimental data were analyzed using Langmuir, Freundlich, Dubinin–Radushkevich and Temkin isotherm models and it was found that the Langmuir model presented a better fit. SEM–EDS confirmed the presence of Zn(II), Cu(II), Pb(II) and Cd(II) ions on the biomass surface. Temperature affects the biosorption process and the thermodynamic parameters show the spontaneous character of the sorption reaction. All energy values obtained are higher than 8 kJ mol$^{-1}$, which implied that Zn(II), Cu(II), Pb(II) and Cd(II) were mainly adsorbed chemically onto the seaweed. The results suggest that the differences in the metal adsorption behavior are due to the different metal affinities to the cell wall polysaccharides.

Removal of heavy metal ions, in particular Pb(II) and Cd(II), by *G. torulosus* seems to be an efficient and low cost alternative technology to be considered in industrial effluent treatment. The development of this technology for polluted effluents purification would likely increase seaweed demand and consequently increase the economies of the countries that produce this good.

## Acknowledgements

The authors acknowledge Universidad de Buenos Aires, for financial support through Project UBACyT X043, Secretaria de Ciencia y Técnica, Agencia Nacional de Promoción Científica y Tecnológica, SECyT- ANPCyT- FONCyT through PICT 32678 and Consejo Nacional de Investigaciones Científicas y Técnicas de la República Argentina (CONICET). Authors are also grateful to Dr. Marina Ciancia and Dr. José Estevez for providing the seaweed used for this research.

## References

[1] A.J.P. Esteves, E. Valdman, S.G.F. Leite, Repeated removal of cadmium and zinc from an industrial effluent by waste biomass *Sargassum* sp., Biotechnol. Lett. 22 (2000) 499–502.
[2] P. Lodeiro, J.L. Barriada, R. Herrero, M.E. Sastre de Vicente, The marine macroalga *Cystosira baccata* as biosorbent for cadmium(II) and lead(II) removal: kinetic and equilibrium studies, Environ. Pollut. 142 (2006) 264–273.
[3] E. Harry, Treatment of metal-contaminated wastes: why select a biological process, Trends Biotechnol. 17 (1999) 462–465.
[4] P. Miretzky, A. Saralegui, A. Fernandez Cirelli, Simultaneous heavy metal removal mechanism by dead macrophytes, Chemosphere 62 (2006) 247–254.
[5] B. Volesky, Sorption and Biosorption, BV-Sorbex Inc., Quebec, Canada, 2003.
[6] B. Volesky, Z.R. Holan, Biosorption of heavy metals, Biotechnol. Prog. 11 (1995) 235–250.
[7] T.A. Davis, B. Volesky, R.H.S.F. Vieira, Sargassum seaweed as biosorbent for heavy metals, Water Res. 34 (2000) 4270–4278.
[8] P. Donghee, Y. Yeoung-Sang, A. Chi Kyu, P. Jong Moon, Kinetics of the reduction of hexavalent chromium with the brown seaweed Ecklonia biomass, Chemosphere 66 (2007) 939–946.
[9] M.M. Areco, E. Valdman, M. dos Santos, Afonso, Zinc biosorption by seaweed illustrated by the zincon colorimetric method and the langmuir isotherm, J. Chem. Educ. 84 (2007) 302–305.
[10] A. Sari, M. Tuzen, Biosorption of Pb(II) and Cd(II) from aqueous solution using green alga (Ulva lactuca) biomass, J. Hazard. Mater. 152 (2008) 302–308.
[11] B. Jha, S. Basha, S. Jaswar, B. Misrha, M.C. Thakur, Biosorption of Cd(II) and Pb(II) onto brown seaweed, *Lobophora variegata* (Lamouroux): kinetics and equilibrium studies, Biodegradation 20 (2009) 1–13.
[12] L. Deng, Y. Zhang, J. Qin, X. Wang, X. Zhu, Biosorption of Cr(VI) from aqueous solutions by nonliving green algae *Cladophora albida*, Miner. Eng. 22 (2009) 372–377.
[13] M.C. Basso, A.L. Cukierman, Biosorption performance of red and green marine macroalgae for removal of trace cadmium and nickel from wastewater, Int. J. Environ. Pollut. 34 (2008) 340–352.
[14] G.J. Ramelow, D. Fralick, Y. Zhao, Factors affecting the uptake of aqueous metal ions by dried seaweed biomass, Microbios 72 (1992) 81–93.
[15] D. Roy, P.N. Greenlaw, B.S. Shane, Adsorption of heavy metals by green algae and ground rice hulls, J. Environ. Sci. Health—Part A. Environ. Sci. Eng. 28 (1993) 37–50.
[16] Z.R. Holan, B. Volesky, Biosorption of lead and nickel by biomass of marine algae, Biotechnol. Bioeng. 43 (1994) 1001–1009.
[17] E. Valdman, L. Erijman, F.L.P. Pessoa, S.G.F. Leite, Continuous biosorption of Cu and Zn by immobilized waste biomass Sargassum sp, Process Biochem. 36 (2001) 869–873.

[18] S.O. Prasher, M. Beaugeard, J. Hawari, P. Bera, R.M. Patel, S.H. Kim, Biosorption of heavy metals by red algae (*Palmaria palmata*), Environ. Technol. 25 (2004) 1097–1106.
[19] A. Saeed, M. Iqbal, M.W. Akhtar, Removal and recovery of lead(II) from single and multimetal (Cd, Cu, Ni, Zn) solutions by crop milling waste (black gram husk), J. Hazard. Mater. 117 (2005) 65–73.
[20] V. Murphy, H. Hughes, P. McLoughlin, Enhancement strategies for Cu(II), Cr(III) and Cr(VI) remediation by a variety of seaweed species, J. Hazard. Mater. 166 (2009) 318–326.
[21] A.B. Ariff, M. Mel, M.A. Hasan, M.I.A. Karim, The kinetics and mechanism of lead (II) biosorption by powderized *Rhizopus oligosporus*, World J. Microbiol. Biotechnol. 15 (1999) 291–298.
[22] A. Van der Wal, W. Norde, J.B. Zhnder, J. Lyklema, Determination of the total charge in the cell walls of Gram-positive bacteria, Colloids Surf. B 9 (1997) 81–100.
[23] A. Esposito, F. Paganelli, F. Veglio, pH related equilibria models for biosorption in single metal systems, Chem. Eng. Sci. 57 (2002) 307–313.
[24] E. Valdman, S.G.F. Leite, Biosorption of Cd, Zn and Cu by *Sargassum* sp. waste biomass, Bioprocess Eng. 22 (2000) 171–173.
[25] S. Kalyani, P. Srinivasa Rao, A. Krishnaiah, Removal of nickel (II) from aqueous solutions marine macroalgae as the sorbing biomass, Chemosphere 57 (2004) 1225–1229.
[26] A.I. Ferraz, A.I. Tavares, J.A. Teixeira, Cr(III) removal and recovery from *Saccharomyces cerevisiae*, Chem. Eng. J. 105 (2004) 11–20.
[27] R. Gong, Y. Ding, H. Liu, Q. Chen, Z. Liu, Lead biosorption and desorption by intact and pretreated spirulina maxima biomass, Chemosphere 58 (1995) 125–130.
[28] A. Saeed, M.W. Akhtar, M. Iqbal, Affinity relationship of heavy metal biosorption by the husk of *Cicer arientinum* (Chickpea var. black gram) with their atomic weights and structural features, Fresenius Environ. Bull. 14 (2005) 219–223.
[29] T.T.T.B.R. Vijayaraghavan, K.U.M. Joshi, Application of *Sargassum* biomass to remove heavy metal ions from synthetic multi-metal solutions and urban storm water runoff, J. Hazard. Mater. 164 (2009) 1019–1023.
[30] I.A. Şengil, M. Özacar, Competitive biosorption of Pb2+, Cu2+ and Zn2+ ions from aqueous solutions onto valonia tannin resin, J. Hazard. Mater. 166 (2009) 1488–1494.
[31] E.C. Ormerod, A.C.D. Newman, Water sorption on Ca saturated clays: II. Internal and external surfaces of mortmorillonite, Clay Miner. 18 (1983) 289–299.
[32] R.M. Torres Sánchez, S. Falasca, Specific surface area and surface charges of some argentinian soils, Zeitschrift für Pflanzenernährung und Bodenkunde 160 (1997) 223–226.
[33] J.A. Platte, V.M. Marcy, Photometric determination of zinc with zincón, Anal. Chem. 31 (1959) 1226–1228.
[34] Y.S. Ho, A.E. Ofomaja, Pseudo-second-order model for lead ion sorption from aqueous solutions onto palm kernel fiber, J. Hazard. Mater. B129 (2006) 137–142.
[35] A.K. Bhattacharya, C. Venkobachar, Removal of cadmium (II) by low cost adsorption, J. Environ. Eng. ASCE 110 (1984) 110–122.
[36] Y.S. Ho, G. McKay, Pseudo-second order model for sorption processes, Process Biochem. 34 (1999) 451–465.
[37] P. Solari, A.I. Zouboulis, K.A. Matis, G.A. Stalidis, Removal of toxic metal by biosorption onto nonliving sewage sludge, Sep. Sci. Technol. 31 (1996) 1075–1092.
[38] P. Miretzky, C. Muñoz, A. Carrillo-Chavez, Cd (II) removal from aqueous solution by *Eleocharis acicularis* biomass, equilibrium and kinetic studies, Bioresour. Technol. 101 (2010) 2637–2642.
[39] Y.S Ho, G. McKay, Sorption of dyes and copper ions onto biosorbents, Process Biochem. 38 (2003) 1047–1061.
[40] Q. Li, L. Chai, Z. Yang, Q. Wang, Adsorption onto modified spent grain from aqueous solutions, Appl. Surf. Sci. 255 (2009) 4298–4303.
[41] E. Fourest, A. Serre, J.C. Roux, Contribution of carboxyl groups to heavy metal binding sites in fungal wall, Toxicol. Environ. Chem. 54 (1996) 1–10.
[42] J.L. Gardea-Torresdey, M.K. Becker-Hapak, J.M. Hosea, D.W. Darnall, Effect of chemical modification of algal carboxyl groups on metal ion binding, Environ. Sci. Technol. 24 (1990) 1372–1378.
[43] H. Liu, H.H.P. Fang, Characterization of electrostatic binding sites of extracellular polymers by linear programming analysis of titration data, Biotechnol. Bioeng. 80 (2002) 806–811.
[44] M.J. Brown, J.N. Lester, Role of bacterial extracellular polymers in metal uptake in pure bacterial culture and activated sludge-II, Water Res. 16 (1982) 1549–1560.
[45] E. Fourest, C. Canal, J.C. Roux, Improvement of heavy metal biosorption by mycelial dead biomasses (*Rhizopus arrhizus*, *Mucor miehe*i and *Penicillium chrysogenum*): pH control and cationic activation, FEMS Microbiol. Rev. 14 (1994) 325–332.
[46] M.M. Figueira, B. Volesky, H.J. Mathieu, Instrumental analysis study of iron species biosorption by *Sargassum* biomass, Environ. Sci. Technol. 33 (1999) 1840–1846.
[47] W. Stumm, J.J. Morgan, Chemistry of the Solid–Water Interface, John Wiley & Sons, USA, 1992.
[48] T.A. Davis, B. Volesky, A. Mucci, A review of the biochemistry of heavy metal biosorption by brown algae, Water Res. 37 (2003) 4311–4330.